MOLECULAR AND CELLULAR BIOLOGY, Mar. 1991, p. 1419–1430
0270-7306/91/031419-12$02.00/0

Vol. 11, No. 3

Relationship of Avian Retrovirus DNA Synthesis to Integration In Vitro

YOUNG M. HA LEE AND JOHN M. COFFIN*

Department of Molecular Biology and Microbiology, Tufts University School of Medicine, 136 Harrison Avenue, Boston, Massachusetts 02111

Received 1 August 1990/Accepted 10 December 1990

An in vitro integration system derived from avian leukosis virus-infected cells supports both intra- and intermolecular integration of the viral DNA. In the absence of polyethylene glycol, intramolecular integration of viral DNA molecules into themselves (autointegration) was preferred. In the presence of polyethylene glycol, integration into an exogenously supplied DNA target was greatly promoted. Analysis of integration intermediates revealed that the strand transfer mechanisms of both reactions were identical to those of retroviruses and some transposons: each 3′ end of the donor molecule is joined to a 5′ end of the cleaved target DNA. The immediate integration precursor appears to be linear viral DNA with the 3′ ends shortened by 2 nucleotides. Finally, in the avian system, most cytoplasmic viral DNA appears to be incomplete and further DNA synthesis is required for integration in vitro.

Early events in retrovirus replication include two unique events: synthesis of a double-stranded DNA copy of the viral RNA genome and integration of this DNA into cellular DNA to form a provirus (for review, see references 16 and 33). These processes occur within the context of a nucleoprotein structure derived from the viral capsid (3, 4). The organization of this structure is poorly understood, but it seems to contain at least the major capsid (CA) protein, as well as reverse transcriptase and integrase (IN) activities necessary for the corresponding reactions.

The process of viral DNA synthesis has been studied for some time. To summarize briefly, internally primed initiation of both plus- and minus-strand DNA synthesis followed by transfer of the growing chains to complementary sequences at the other end of the genome leads to a double-stranded linear molecule. This molecule has at its ends long terminal repeat (LTR) sequences in which substantial regions of the viral genome (U3 and U5) have been duplicated around copies of the short repeat (R) found at either end of the genome. Minus-strand synthesis is initiated at the 3′ end of the tRNA primer and extended to the 5′ end of the genome to form a structure called minus-strong-stop DNA. Extension of this strong-stop DNA from the 3′ end of the genome (after removal of R-U5 by RNase H and base-pairing with the R sequence at the 3′ end of the genome) permits completion of most of the minus strand. Initiation of plus-strand DNA synthesis occurs with the specifically nicked genome RNA as the primer (12, 24, 30), copying the U3, R, and U5 sequences of the minus strand and 18 nucleotides of the tRNA primer (15, 26, 32). This forms a structure called plus-strong-stop DNA. Transfer of this molecule to the other end of minus-strand DNA permits completion of both strands.

With some retroviruses, such as mouse mammary tumor virus (21), plus-strand synthesis is initiated at only one point, the 5′ end of the plus-strong-stop sequence. With others, such as avian leukosis virus (ALV), there seem to be multiple points of initiation of plus-strand synthesis, leading to a variety of short fragments, which seem to eventually be displaced by full-length molecules (2, 17, 18, 21). The majority of unintegrated viral DNA molecules in ALV-infected cells have been found to contain nearly full-length minus strands and fragmentary plus strands, even at late times after infection.

The mechanisms of retroviral integration have been partially elucidated by the recent development of in vitro integration systems (4–6, 8, 11, 13, 14, 19). The weight of existing evidence favors a model in which two nucleotides are removed from each complete 3′ end of the linear viral DNA and the recessed 3′ ends are joined to the 5′ ends of target DNA subsequent to its cleavage. It has been shown that the cleavage and joining reactions of integration can be carried out by the IN protein by using short oligonucleotides with terminal LTR sequences and that these events may be energetically coupled, at least in the in vitro integration system (6, 8, 19). Cellular repair systems could then fill in the staggered ends of the target DNA.

We have recently described the development of an in vitro integration system for an ALV (21a). This system uses viral DNA-protein structures derived from acutely infected cells, similar to a system reported for murine leukemia virus (MLV) (4). However, unlike MLV, the ALV-derived particles direct highly efficient autointegration, in which the viral DNA molecule integrates into itself, giving rise to circular forms of viral DNA.

In the present study, we have analyzed the viral DNA in this in vitro integration system. Most of the unintegrated viral DNA molecules in ALV-infected cells are in the form of incomplete molecules which are completed during the in vitro integration reaction. Moreover, it appears that most integration events observed in vitro are carried out by the newly synthesized viral DNA. We have also found that the ALV system will catalyze efficient integration of viral DNA into exogenous target DNA in the presence of polyethylene glycol (PEG). Results from the analyses of the viral DNAs also indicate that linear DNA with 2-nucleotide recessed ends is the integration precursor.

* Corresponding author.

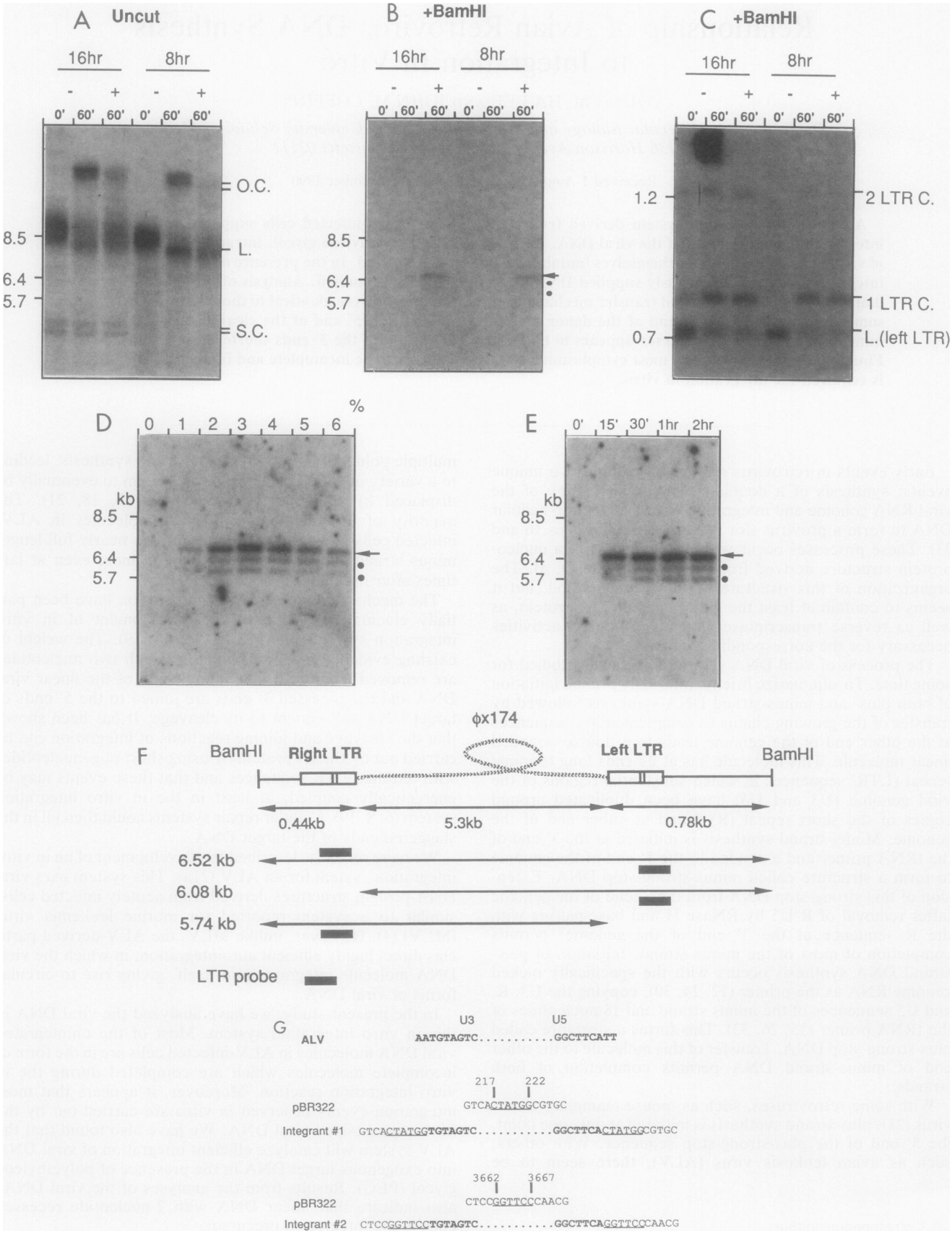
A Uncut
16hr
8hr
- + - +
0' 60' 60' 0' 60' 60'
O.C.
L.
S.C.
8.5
6.4
5.7
B +BamHI
16hr
8hr
- + - +
0' 60' 60' 0' 60' 60'
8.5
6.4
5.7
C +BamHI
16hr
8hr
- + - +
0' 60' 60' 0' 60' 60'
1.2
0.7
2 LTR C.
1 LTR C.
L.(left LTR)
D
0 1 2 3 4 5 6 %
kb
8.5
6.4
5.7
E
0' 15' 30' 1hr 2hr
kb
8.5
6.4
5.7
F
φx174
BamHI
Right LTR
Left LTR
BamHI
0.44kb
5.3kb
0.78kb
6.52 kb
6.08 kb
5.74 kb
LTR probe
G
U3
U5
ALV
AATGTAGTC.....GGCTTCATT
217
222
pBR322
GTCACTATGGCGTGC
Integrant #1
GTCACTATGGTGTAGTC.....GGCTTCACTATGGCGTGC
3662
3667
pBR322
CTCCGGTTCCCAACG
Integrant #2
CTCCGGTTCCTGTAGTC.....GGCTTCAGGTTCCCAACG

MATERIALS AND METHODS

Cells and viruses. QT6 cells are a continuous line derived from a methylcholanthrene-induced fibrosarcoma of Japanese quail (23). CS8 virus is a derivative of Rous sarcoma virus (RSV)-PrC containing a bacterial suppressor tRNA inserted in place of *src* and is replication competent (29). To make an acutely infected cell extract, QT6 cells were infected with fresh viral supernatant prepared from turkey embryo fibroblasts chronically infected with CS8.

In vitro integration reaction conditions. Cell extracts were prepared 8 or 16 h after infection of QT6 cells with CS8. The plates were washed twice with ice-cold hypotonic buffer (20 mM HEPES [*N*-2-hydroxyethylpiperazine-*N'*-2-ethanesulfonic acid, pH 7.5], 5 mM KCl, 1 mM dithiothreitol, 1 mM $MgCl_2$). After a second wash, residual fluid was removed with a Pasteur pipette into a Dounce homogenizer, and the cells were scraped off the plates and lysed by 20 strokes with a tight-fitting pestle. Cell debris was removed by centrifugation at 20,000 × *g* for 20 min, and the supernatant (extract) was used for all further experiments. A standard reaction mixture (0.2-ml total volume) for in vitro integration contained 50 mM HEPES (pH 7.5), 7 mM $MgCl_2$, 1 mM dithiothreitol, 100 mM KCl, 1 mM ATP, 10 mM creatine phosphate, 50 μg of creatine phosphokinase, 50 mM deoxynucleotide triphosphates, 0.1 mg of bovine serum albumin per ml, and 0.5 to 1 μg of φX174 replicative form I (RFI) DNA. The in vitro integration reaction was carried out at 30°C for 1 h. Although it has been shown that a high energy cofactor is not necessary for the integration reaction with MLV (4), we included such factors because we have not yet defined the external energy requirement for our in vitro integration reaction. The reaction was stopped by the addition of 20 mM EDTA–0.2% pronase–0.5% sodium dodecyl sulfate (SDS) and incubation at 37°C for 1 h. The DNA was isolated by phenol-chloroform (1:1), phenol, and phenol-chloroform (1:1) extractions and subsequent ethanol precipitation. For efficient integration into the target DNA, PEG 8000 (Sigma) was added at 3% (wt/vol).

Gel electrophoresis. Agarose gel electrophoresis was carried out in 0.1 M Tris-borate–2 mM EDTA. Denaturing agarose gel electrophoresis was done as described by Maniatis et al. (22). The agarose gel was equilibrated in 30 mM NaOH–1 mM EDTA before electrophoresis, and electrophoresis was done at 5 to 7 V/cm in the same buffer. DNA samples were precipitated with ethanol, dried, and resuspended in denaturing sample buffer (50 mM NaOH, 1 mM EDTA, 2.5% Ficoll, 0.25% bromocresol green). For analysis of the ends of viral DNA, DNA samples were incubated with appropriate restriction enzymes, ethanol precipitated, dissolved in 5 μl of loading buffer (80% formamide, 0.05% bromophenol blue, 0.05% xylene cyanol, 1 mM EDTA), denatured by heating at 90°C for 2 min, and subjected to urea-polyacrylamide gel electrophoresis (7 M urea, 0.1 M Tris-borate, 2 mM EDTA).

Southern transfers and hybridization. DNA was transferred to Zetabind nylon membranes (Cuno) by the standard capillary transfer method for agarose gels (22). DNAs analyzed in polyacrylamide were transferred onto Zetabind membranes by the electroblotting method suggested by the manufacturer (Hoeffer Scientific). Nondenaturing agarose gels were first treated with HCl for 15 to 20 min, denatured with 1 N NaOH–0.5 M NaCl for 30 to 60 min, and transferred onto the membrane with 20× SSC (3 M NaCl, 0.3 M sodium citrate, pH 7.0). Alkaline denaturing gels were transferred directly with 20× SSC without further treatment. After transfer, the membranes were treated with 0.4 N NaOH to fix the DNA to the membrane, neutralized with Tris-HCl (pH 7.5), equilibrated with 2× SSC, air-dried, and baked at 80°C in vacuo. The hybridization conditions were as described by Church and Gilbert (7) with minor modifications. Both prehybridization and hybridization were carried out at 42°C with 0.25 M NaCl–0.25 M sodium phosphate (pH 7.0)–1 mM EDTA–7% SDS–1% bovine serum albumin–50% formamide.

RNA probes. RNA probes were synthesized by using SP6 or T7 RNA polymerase from plasmid DNAs digested with the appropriate restriction enzyme. Probes were gel purified and used at 1×10^6 to 5×10^6 cpm/ml of hybridization solution. Nucleotide designations are those for RSV-PrC (27). The plasmid pSAH3ΔSmB (constructed by Steve Herman) was used to make a (−)RU5 probe. It contained the *Eco*RI (nucleotide [nt] −53) to *Bst*EII (nt 103) fragment of NY203 (28) in the pSP64 vector (Promega). pSAH3ΔS-2, which was used for the (+)RU5 probe, contained the same insert as pSAH3ΔSmB in the opposite orientation in pSP65 (Promega). The U3-containing plasmids pYLU3(+) and pYLU3(−) were constructed by cloning the *Eco*RI fragment of CS8 (from the polylinker site of πAN7 to nt 9238) into the Bluescribe vector (Stratagene). Transcription of plasmids pYLU3(−) and pYLU3(+) with T7 RNA polymerase gives rise to probes representing the minus and plus strands of U3, respectively. The minus-strand-specific leader probe was synthesized from a plasmid, pYL-BS, containing the *Bst*EII

FIG. 1. Intermolecular integration of viral DNA into target DNA in the presence of PEG. Cytoplasmic extracts were prepared 8 or 16 h after infection with CS8. The standard reaction was carried out with φX174 RFI DNA as the target in the absence (−) or presence (+) of 3% (wt/vol) PEG. Before (0′) or after (60′) reaction for 60 min, total DNA was analyzed by agarose gel electrophoresis, transferred onto nylon membranes, and hybridized with an LTR-specific probe [(−)RU5] shown in Fig. 3F. (A) Total DNA analyzed without digestion. (B and C) Total DNA from the reaction in panel A cut with *Bam*HI; (B) upper part of the blot; (C) lower part. (D and E) Total reaction products were analyzed after digestion with *Bam*HI. The products of integration into the φX174 target were identified by hybridization with a viral LTR-specific RNA probe, (−)RU5. (D) To test the optimum concentration of PEG, standard reactions with various concentrations (percent) of PEG were carried out for 60 min at 30°C. (E) Time course (minutes and hours) of integration into the φX174 target in the presence of 3% PEG. (F) Sizes expected for various products of integration into φX174 DNA. Arrows in panels B, D, and E indicate the size expected for complete integration products, and the dots in panels D and E indicate the sizes expected for partial integration products with either of the LTRs joined to the target. Partial integration products were present in the gel shown in panel B but are not visible in the reproduction shown. (G) Integration junction sequences. A reaction similar to that shown in panel A was run with 3% PEG and pBR322 DNA as the target. Reaction products containing the complete plasmid plus both LTRs were cloned in λAS4 (29) after digestion with *Sac*I, which cleaves near each LTR and not in the plasmid DNA. The nucleotide sequence of the two integration joints was determined after subcloning the plasmid-virus sequences and compared with the sequence of the PrC strain of RSV (27) and pBR322 (31). The target site duplications are underlined, and joining viral sequences are shown in boldface. Abbreviations: O.C., open circular viral DNA; L., linear viral DNA; S.C., supercoiled viral DNA; 2 LTR C., two-LTR circular viral DNA; 1 LTR C., single-LTR circular viral DNA.

(nt 103) to *Sac*I (nt 255) fragment of NY203 in the pSP65 vector.

RESULTS

PEG promotes efficient intermolecular integration. Previously, we found that viral DNA structures contained in cytoplasmic extracts from cells infected with ALV mediated efficient integration of the viral DNA into itself (autointegration) but were extremely inefficient at directing integration of the DNA into exogenously supplied target DNA molecules. We reasoned that the inefficiency of the latter reaction might be due to a relatively low effective concentration of reaction components. Therefore, we attempted to increase this concentration by addition of a hydrophilic polymer, PEG.

To study the PEG effect, covalently closed circular DNA, RFI of bacteriophage φX174, was used as a target for viral integration, and cell extracts made at 8 and 16 h after infection were tested. Integration of viral DNA into the φX174 DNA target was detected by hybridization with a viral LTR-specific RNA probe after agarose gel electrophoresis. Integration into the φX174 DNA target should yield a circular molecule of target DNA with the viral DNA inserted. Digestion with a restriction enzyme such as *Bam*HI, which cleaves viral DNA near the ends but does not cleave φX174 DNA, should yield a characteristic fragment consisting of full-length linear target DNA with viral fragments at each end (Fig. 1F).

Addition of PEG greatly stimulated integration of viral DNA into the exogenous target φX174 DNA (Fig. 1). First, total DNA was analyzed without digestion (Fig. 1A). In the absence of PEG, a doublet with the mobility of open circular viral DNA appeared after the reaction (lanes 60′). We have recently shown that the doublet contained both autointegration products and single-LTR circles (21a). In the presence of PEG, more slowly migrating species with heterogeneous gel mobility, possibly the result of topological heterogeneity of the circular integration products, appeared (not visible in the reproduction), and a substantial reduction in the amount of open circular forms was seen. However, digestion of the reaction products with *Bam*HI yielded a sharp band with a mobility consistent with that expected for products of integration into φX174 DNA target (Fig. 1B, arrow). In the absence of PEG, integration into the exogenous target was not detectable by this technique. Examination of the small LTR-containing forms after *Bam*HI digestion (Fig. 1C) revealed a significant decrease in linear forms and an increase in single-LTR circles during the reaction independent of the addition of PEG.

Subsequent cloning, restriction enzyme analysis, and sequencing of two of the reaction products (Fig. 1G) revealed that integration in the presence of PEG was correct; the viral DNA had the expected structure and the sequence rearrangements previously shown to characterize ALV integration, i.e., a loss of 2 nucleotides from each end of the viral DNA and a duplication of 6 nucleotides at the integration site.

The efficiency of intermolecular integration was dependent on the PEG concentration and was maximal at 3% (wt/vol) PEG (Fig. 1D). Most integration occurred within 30 min, but the reaction continued slowly for 1 h (Fig. 1E). Other than PEG, the same reaction conditions were required for intermolecular integration and autointegration (data not shown). We estimated that, on average, about 10% of the viral DNA in the reaction mix integrated into the target DNA at optimum reaction conditions. The much greater reduction in linear forms (Fig. 1A) might reflect integration into random fragments of cell DNA present in the reaction.

In addition to the band corresponding to the integration product of viral DNA into the φX174 DNA target, we routinely observed two minor DNA forms which cross-hybridized with the LTR probe (Fib. 1B, D, and E, indicated by dots). These structures were about 500 or 800 bp smaller than the expected size of the fragment containing two ends of viral DNA joined to φX174 target DNA. Since *Bam*HI cleaves linear viral DNA about 500 bp from the 3′ end and about 800 bp from the 5′ end (Fig. 1G), we postulated that the two smaller structures were incomplete integration products with only one LTR joined to the target. Additional restriction digestion confirmed this interpretation (data not shown).

The time course of integration in the presence of PEG (Fig. 1E) revealed that the amount of DNA in the minor bands was constant relative to the complete integration products and that the relative amounts of the aberrant products with each LTR were the same. This relationship suggested that the minor DNA species were not likely to be active intermediates to complete integration. The migration pattern of integration products with only one LTR was consistent with that expected for double-stranded linear DNA, indicating that both strands of the target DNA were cleaved. We did not observe any forms with a mobility consistent with that expected for an open circle with an LTR-length "tail," the expected product of a joining and cleavage of one strand only.

Immediate integration precursor is linear DNA with 2 nucleotides recessed at the 3′ ends. It has been shown in other in vitro integration systems that the system catalyzes joining of the 3′ ends but not the 5′ ends of the viral DNA to the target DNA (4, 5, 13, 14). It was therefore of interest to analyze whether the same events occur during our in vitro integration reaction. For this purpose, the isolated products of both integration into the exogenous target and autointegration were analyzed in a denaturing polyacrylamide gel, and the ends of the viral DNA were visualized by hybridization with strand-specific LTR probes (Fig. 2). The products of integration into φX174 (lanes a) were isolated by extracting the fragment of the expected size from a low-melting-point agarose gel. Autointegration products (lanes b) were isolated by purifying the heterogeneous fragments in the range of 3 to 7 kb after *Sac*I digestion. LTR-containing fragments from this region should consist largely of autointegration products, since all other forms (ends of the linear DNA and junctions of other circular forms) yield fragments of less than 1.5 kb (the size of the LTR-containing fragment of two-LTR circular DNA generated by *Sac*I is about 1.5 kb).

The 3′ ends of both plus and minus strands appeared to be ligated, comigrating with the target DNA larger than 2 kb (arrow), while the 5′ ends remained free (Fig. 2A). When hybridized with minus-strand-specific probes (right panel), a band consistent with the size expected for the free 5′ LTR (corresponding to the 5′ end of the plus strand) was seen, but no free 3′ LTR (corresponding to the 3′ ends of the plus strand) was observed. Similarly, with the plus-strand probe (left panel), the 3′ LTR (corresponding to the 5′ ends of the minus strand) was free from the target, but not the 5′ LTR, indicating that they must be joined to the target. We thus conclude that, as with MLV (5, 13, 14), the integration reaction proceeds by joining the 3′ ends of each LTR to the 5′ ends of the cut target DNA, leaving the other ends free to be repaired and joined in a subsequent step which seems not

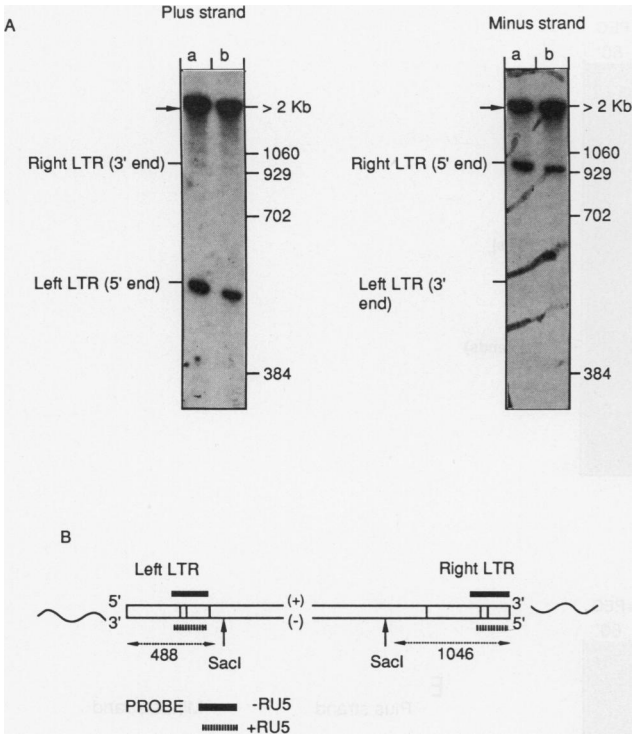

FIG. 2. Products of autointegration and integration into ϕX174 are integration intermediates. (A) To produce products of integration into ϕX174 DNA, a reaction was carried out as described in the legend to Fig. 1 with 3% PEG. Total DNA was digested with *Sac*I, and fragments of the size expected for products of integration into ϕX174 DNA, about 6.5 kb, were isolated from low-melting-point agarose gels (lanes a). Autointegration products were isolated as described in the text (lanes b) after the reaction was carried out without PEG. Both integration products were analyzed in a denaturing 4% polyacrylamide gel and hybridized with the plus-strand-specific LTR probe (left panel, plus strand) and the minus strand-specific LTR probe (right panel, minus strand). (B) Schematic illustration of the structure of integration intermediates if the 3′ ends of ALV donor viral DNA join to the target and the 5′ ends of the donor DNA remain unjoined. The (+) indicates the plus strand and the (−) indicates the minus strand of linear duplex viral DNA.

to occur in vitro. The strand transfer reactions of both inter- and intramolecular integration appeared to be the same.

To study the ends of the viral DNA molecules more closely, the integration intermediate and total viral DNA in the reaction mix were further analyzed by electrophoresis in a high-resolution polyacrylamide gel (Fig. 3). The product of integration into the target ϕX174 RFI DNA was isolated after *Eco*RI restriction digestion (lanes I). Total DNAs were prepared at different reaction times and digested with *Eco*RI before analysis (lanes 0′ to 60′). Each end of viral DNA was visualized by hybridization with specific probes for each of the LTR ends.

Each 5′ end of linear viral DNA in the reaction was a single DNA species whose size was identical to that expected for full-length viral DNA (Fig. 3A and D, 181 and 150 nt, respectively), and the amounts were relatively constant throughout the reaction, indicating that the 5′ ends of the linear viral DNA did not participate in the reaction in vitro. In contrast, the 3′-terminal fragments of each strand (Fig. 3B and C) were always doublets, consisting of both the full-length ends (154 and 185 nt) and 2-base recessed ends (152 and 183 nt). As the reaction proceeded, the recessed 3′ ends disappeared rapidly but the amount of full-length ends showed little change, suggesting that the recessed 3′ ends were involved in the integration reaction and were likely the immediate precursors for integration.

The integration intermediates contained unligated 5′ ends which were the same size as full-length linear molecules (Fig. 3A and D, lanes I), suggesting that the linear form of viral DNA was the integration precursor. If the circular form was the precursor and cleaved by a 4-base staggered cut, the unligated 5′ LTR ends of the integration intermediates would be expected to be 2 nucleotides larger than the full-length linear molecules. The 3′ ends were joined to the target and migrated too slowly to be seen in this analysis (Fig. 3B and C, lanes I). Autointegration intermediates gave the same results (data not shown), confirming again that both inter- and intramolecular integrations follow the same biochemical pathways.

The recessed 3′ ends of the linear viral DNA could have been created either by cleavage of completed ends or by termination of DNA synthesis 2 nucleotides prior to the end. Analysis of viral DNA in extracts prepared at an earlier time after infection (8 h) (Fig. 3E, 0′) revealed more full-length than recessed ends. At later times after infection, i.e., 16 h (Fig. 3B and D, 0′), there were more recessed ends than full-length ends. The result implies that the 2-base recessed ends were likely cleavage products of the full-length viral DNA.

During this study, we detected a 172-nucleotide fragment corresponding to plus-strong-stop DNA (Fig. 3B, +SS), which contained a copy of the 5′ end of the minus-strand DNA as well as 18 nucleotides of the tRNA primer, as previously predicted (15). The very faint 151-nucleotide fragment (Fig. 3D) is likely the minus-strand DNA species with the 3′ ends of the $tRNA^{Trp}$ primer still attached. Since pancreatic RNase cleaves 3′ of pyrimidine nucleotides and the 3′ end of the tRNA primer has the sequence CA, digestion of such minus-strand DNA species would generate molecules 1 nucleotide larger.

The U3 probe also detected a 288-base internal fragment (Fig. 3A and C). The intensity of the hybridization to the internal fragments was greater than that to the end fragments. The lack of the end fragments is more apparent for the 3′ ends (panel C) than for the 5′ ends (panel A). The discrepancy in the 5′ ends was consistent with the extent of complementarity between the probe and the template. All 288 nucleotides of the U3 probe should hybridize to the internal fragments, while only 180 nucleotides should hybridize to the end fragments. However, the reduced intensity of the band corresponding to the 3′ ends was too great to be due to a difference in hybridization efficiency. Further analysis revealed that the 3′ ends of the minus-strand DNA were indeed less abundant than the 5′ ends of the minus strands (discussed below).

Plus strands of viral DNA are synthesized during the in vitro integration reaction. One of the obvious changes observed during the in vitro integration reaction was the mobility of the linear viral DNA. Before the reaction, it was lower than expected, and the band corresponding to the linear viral DNA appeared fuzzy in the gel (Fig. 1A). Following the integration reaction, the amount of linear DNA was reduced, and its mobility was increased and sharpened. We hypothesized that the fuzziness might be due to the heterogeneity caused by incomplete synthesis of the plus strands of linear viral DNA (21) and that viral DNA synthesis during the

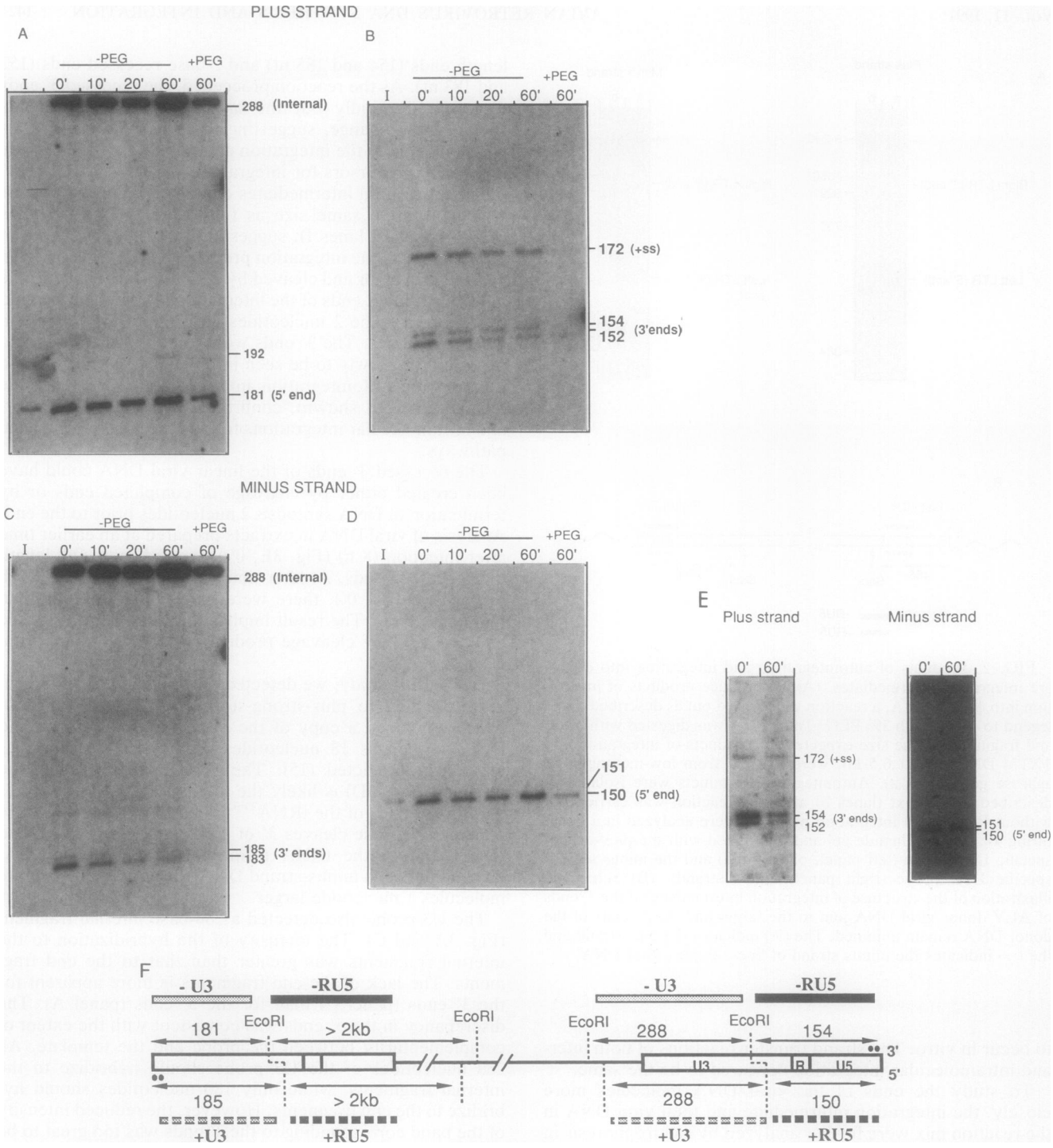

FIG. 3. Ends of the integration products and total viral DNA in the in vitro integration reaction. The products of integration into ϕX174 DNA were isolated as described in the legend to Fig. 2 after reaction in the presence of 3% PEG, except that the DNA was digested with *Eco*RI (lanes I). Total DNAs were prepared after reaction for different times (lanes 0′ to 60′ [0 to 60 min]) in the absence (−) or presence (+) of PEG and digested with *Eco*RI. All samples were treated with pancreatic RNase at the time of restriction enzyme digestion. The samples were then analyzed in a denaturing 6% polyacrylamide gel, transferred onto a nylon membrane, and hybridized with the four different strand-specific LTR RNA probes shown in panel F. Before hybridization with each RNA probe, the blots were stripped by treatment with 1 N NaOH. The size of each DNA band was determined by comparison with sequencing ladders in adjacent lanes of the gels (not shown). (A to D) Extract made 16 h after infection; (E) 8-h extract. (A) The Southern blot was hybridized with a (−)U3 probe to detect 5′ ends of plus strands. This probe also detects a 288-nucleotide fragment containing U3 and some internal sequences, as shown in panel F. (B) Hybridization with a (−)RU5 probe to detect 3′ ends of plus strands. This probe also detects a 172-nucleotide fragment corresponding to the plus-strong-stop DNA (+SS). (C) Hybridization with a (+)U3 probe to detect 3′ ends of minus strands. This probe also detects the 288-nucleotide fragment, as shown in panel F. (D) Hybridization with a (+)RU5 probe to detect 5′ ends of minus strands. This probe also detects the 151-nucleotide fragment which is likely to be the minus-strand DNA species with the 3′ A residue of the $tRNA^{Trp}$ primer still attached. (E) An extract was made 8 h after infection, and reactions were carried out without PEG. Total reaction products were analyzed as before. The blot was hybridized either with a (−)RU5 probe (left panel) or with a (+)RU5 probe (right panel). (F) Cartoon indicating the probes used and fragments detected.

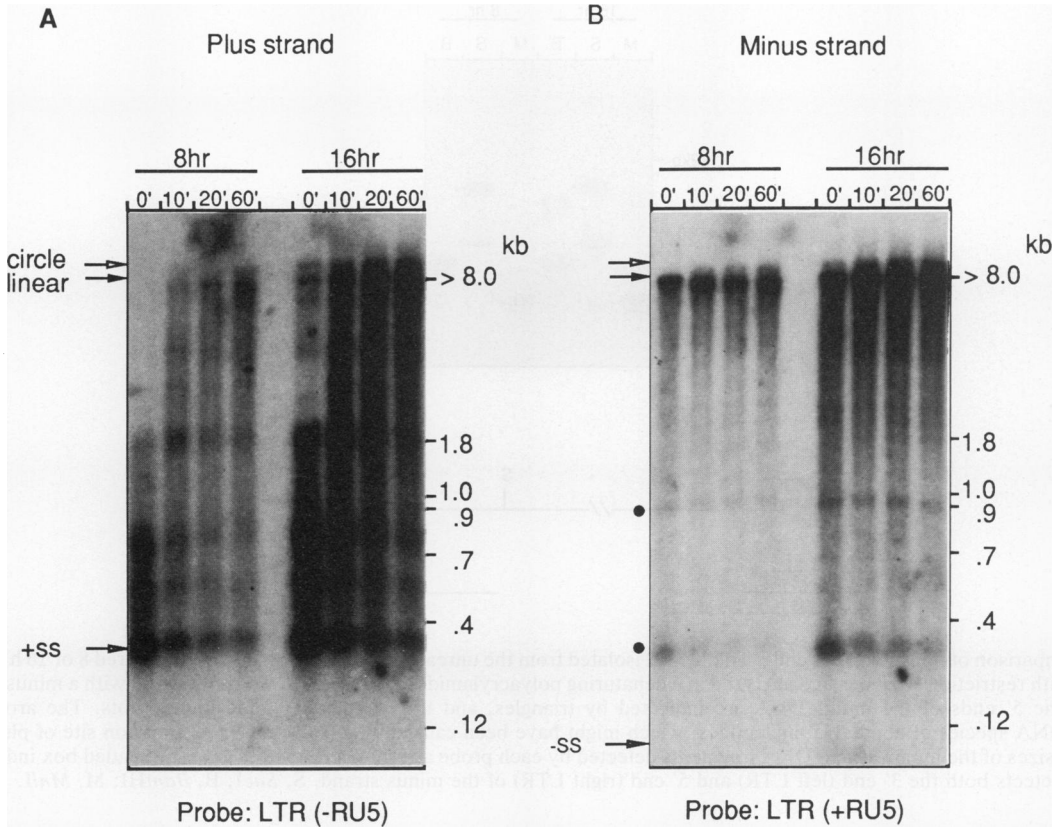

FIG. 4. Alkaline agarose gel analysis of viral DNA during the in vitro reaction. Extracts were prepared 8 to 16 h after infection, and the reactions were carried out without PEG. Total DNA was isolated after different reaction times and analyzed by alkaline agarose gel electrophoresis. The plus- and minus-strand DNAs were identified by hybridization with strand-specific LTR probes (A and B, left and right panels, respectively). The LTR probes are shown in Fig. 3F. +SS, Plus-strong-stop DNA.

reaction might have resulted in the altered migration pattern of the DNA. To investigate this hypothesis, total viral DNA from the in vitro integration reaction was prepared at different times and analyzed by denaturing agarose gel electrophoresis (Fig. 4). The plus (Fig. 4A) and minus (Fig. 4B) strands were visualized by hybridization with strand-specific LTR probes.

Such analysis revealed that before the reaction, most of the plus strands of the viral DNA were mixtures of smaller fragments (Fig. 4A). Following the reaction, the smaller plus strands disappeared as full-length strands appeared. Hybridizing the same blot with internal probes revealed the presence of plus-strand fragments which were initiated internally and did not contain LTR sequences. The overall changes in these molecules were very similar to those of LTR-containing molecules (data not shown). However, the majority of minus strands (Fig. 4B) were approximately full length (linear), and the minus strands showed little change throughout the reaction. This result confirmed our hypothesis that plus-strand DNA synthesis was occurring during the in vitro integration reaction.

The time course of plus-strand synthesis during the in vitro integration reaction (Fig. 4A) revealed that maturation of the plus strand correlated with the appearance of the circles resulting from autointegration as well as formation of single-LTR circles (circles). We also observed previously that the mobility changes of the linear viral DNA coincided with the appearance of the autointegration products (21a). This suggested that the integration reaction was closely associated with plus-strand DNA synthesis.

During this analysis, we found at least two discrete minus-strand DNA forms (Fig. 4B, indicated by dots), which might be caused by a pause during reverse transcription, and at most a trace amount of minus-strong-stop DNA (−SS, faint fuzzy band at the bottom of the gel). The lower band appeared to contain only LTR sequences (data not shown) and corresponded to about 335 nucleotides in another analysis (Fig. 5). The size of this fragment indicates that the pause site must be at the end of U3, just before the polypurine tract.

Minus-strand DNA synthesis is incomplete. Although the results in Fig. 4 showed that minus strands were approximately full length, the previous analysis (Fig. 3) revealed that the 3′-terminal fragments (185 and 183 nt) of the minus strands appeared to be present at lower concentrations than the internal fragments (288 nt). To test whether the ends of the minus strands were completely synthesized, further analysis was carried out. The total DNA before the reaction was digested with several different enzymes, and both the 3′ ends and the 5′ ends of the minus strands were compared after hybridization with a minus-strand-specific LTR probe. Since it was possible that the enzyme sites might be single stranded due to incomplete plus-strand synthesis, we also used *MnlI*, which cleaves single-stranded DNA 50% as efficiently as it does double-stranded DNA. The results are shown in Fig. 5.

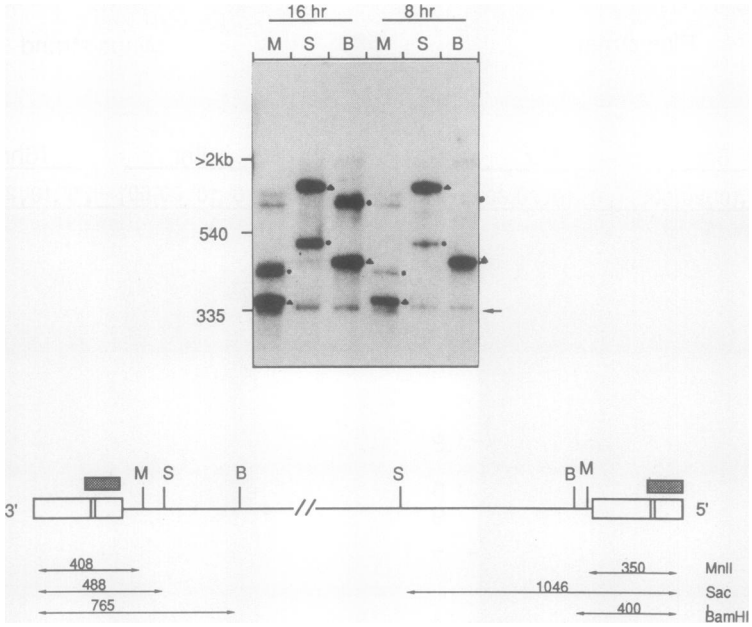

FIG. 5. Comparison of minus-strands ends. Total DNA isolated from the unreacted extracts, which were prepared 8 or 16 h after infection, was digested with restriction enzymes and analyzed in a denaturing polyacrylamide gel. The DNA was hybridized with a minus-strand-specifc LTR probe. The 5′ ends of the minus DNA are indicated by triangles, and the 3′ ends are indicated by dots. The arrow indicates a minus-strand DNA species of about 335 nucleotides, which might have been caused by a pause near the initiation site of plus-strand DNA synthesis. The sizes of the minus-strand DNA fragments detected by each probe are shown below the gel. The shaded box indicates the LTR probe, which detects both the 3′ end (left LTR) and 5′ end (right LTR) of the minus strand. S, *Sac*I; B, *Bam*HI; M, *Mnl*I.

In digests with three different restriction enzymes, the amount of the 5′-end fragments (indicated by triangles) was substantially greater than that of the 3′ ends (indicated by dots), particularly at 8 h after infection. Thus, we concluded that although the minus strands were almost full length, their synthesis might not be completed near the 3′ ends. The fragments of about 335 nucleotides (indicated by the arrow) are the DNA species detected in the alkaline agarose gel analysis (Fig. 4) and are presumed to be generated by a pause near the site of initiation of plus-strand DNA.

Integration reaction in vitro is dependent on viral DNA synthesis. Since the previous experiments revealed that a significant fraction of both plus and minus strands in the extract were not completely synthesized at the time of the in vitro integration reaction, it seemed plausible that viral DNA synthesis might be necessary for integration. We therefore reasoned that 2′,3′-dideoxynucleotides, analogs which terminate DNA elongation, would block viral DNA synthesis and thus integration. For this experiment, an 8-h extract was used because it was as active as the 16-h extract for integration in vitro and we could analyze single-LTR circle formation because of the lack of preexisting circles (Fig. 1).

To test the effects of dideoxynucleotides in the in vitro integration reaction, the reaction was carried out with various concentrations of deoxynucleoside triphosphates (dNTPs) and dideoxynucleoside triphosphates (ddNTPs) (Fig. 6). For analysis of intermolecular integration (Fig. 6A, indicated by the arrow) and single-LTR circle formation (Fig. 6B), the reaction was carried out with 3% PEG and the reaction products were digested with *Bam*HI. As shown in lanes 2 and 3, addition of dNTPs was not necessary for the in vitro integration reaction. This indicates either that the concentrations in the extract were sufficient to allow elongation of plus strands or that dNTPs were generated during the reaction. However, both integration into an exogenous target (Fig. 6A) and formation of single-LTR circles (Fig. 6B) were inhibited by the presence of ddNTPs in the reaction. The inhibition of integration by ddNTP became obvious at concentrations higher than 5 μM and increased as the ddNTP concentration increased. It was also apparent that inhibition of integration by ddNTPs was incomplete even at 50 μM, possibly due to competition with the dNTPs present in the extract or perhaps a low affinity of the reverse transcriptase for ddNTP. The inhibition of the integration reaction by ddNTPs, along with plus-strand synthesis observed during the reaction, strongly indicated that most viral DNA in the extract was not completely synthesized and that further DNA synthesis was required for integration in vitro.

Although the disappearance of some viral DNA could not be accounted for (it may have been due to integration into cellular DNA present in the reaction), the above experiments indicate that viral DNA synthesis is required for integration and that most integration events observed in vitro involve viral DNA which is newly synthesized during the reaction. Despite apparent viral DNA synthesis during the in vitro integration reaction, we have not observed the accumulation of completed 3′ ends of viral DNA (Fig. 3), suggesting that integration occurred shortly after the viral DNA is synthesized and that viral DNA may be a limiting factor for integration.

DISCUSSION

The in vitro integration system developed for an avian retrovirus supports both integration of viral DNA into itself, autointegration (21a), and integration into an exogenous target DNA in the presence of PEG. Since the decrease in

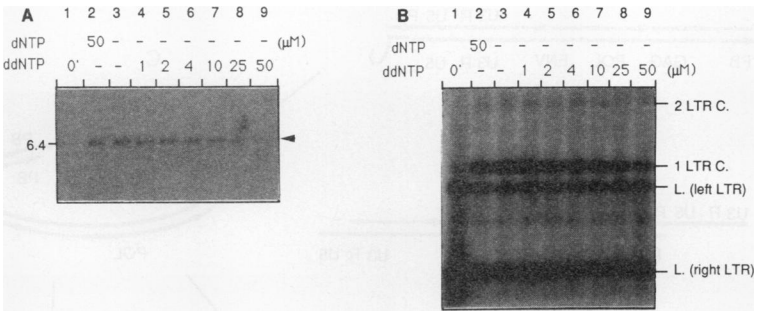

FIG. 6. Inhibition of in vitro integration by ddNTPs. An extract was prepared 8 h after infection. The reactions were carried out under standard reaction conditions in the presence (50 μM) and absence of dNTPs or with increasing (0 to 50 μM) amounts of each ddNTP. The reaction was carried out with 3% PEG, and the reaction products were analyzed in a native agarose gel after digestion with *Bam*HI. The viral DNA before the reaction is represented by 0 min (0'). The (A) Upper part of the gel; (B) lower part of the gel. All were probed with the (−)RU5 probe. The arrowhead indicates the products of integration into the exogenous φX174 target DNA. Abbreviations: 2LTR C., Two-LTR circular viral DNA; 1LTR C., single-LTR circular viral DNA; L., linear viral DNA.

linear forms and the increase in single-LTR circles observed during the reaction were independent of the addition of PEG, the reduction in the amount of open circular forms (Fig. 1A) suggests that integration into exogenous target DNA in the presence of PEG was promoted at the expense of autointegration. The promotion of intermolecular integration at the expense of autointegration in the presence of PEG implies that the effective concentration of a protein(s) or target DNA may determine whether integration occurs inter- or intramolecularly.

Analysis of integration intermediates revealed that each 3′ end of the donor molecule was joined to a 5′ end of the cleaved target DNA and that the immediate integration precursor appeared to be linear viral DNA with 2-nucleotide recessed 3′ ends. Recent reports have shown that cleavage of donor viral DNA ends and correct integration in vitro can be carried out by the purified avian retroviral IN protein (19). The polarity of the strand transfer reaction of avian retrovirus integration was identical to that reported for MLV and human immunodeficiency virus (5, 6, 13, 14), for the transposons Mu (9) and Tn*10* (1), and for the yeast retrotransposon Ty1 (10), providing evidence of the generality of the integration process among insertion elements.

It had previously been reported that in cells infected with avian retroviruses, few full-length plus strands are found, even at late times after infection (21). However, the relationship between viral DNA synthesis and integration has not been investigated. During the detailed analysis of viral DNA in the in vitro integration reaction, we found that most cytoplasmic viral DNA was incapable of integration without further DNA synthesis. Most of the viral DNAs had fragmented plus strands and a deficit of minus-strand 3′ ends. Despite the similarity of the polarity of the integration reactions, avian retrovirus DNA synthesis is clearly different from that of other retroviruses, such as MLV, in which linear viral DNA is completely synthesized in the cytoplasm and is active for integration without further DNA synthesis (4). Figure 7 summarizes the events in viral DNA synthesis and integration that we have observed and inferred from the ALV in vitro integration system.

The major form of viral DNA in the extract is linear DNA with nearly full-length minus strands and fragmented plus strands (Fig. 7A and B). As in other retroviral systems, the majority of minus strands are initiated at one site from the tRNA primer and elongated as a single molecule. In contrast, there are multiple but specific internal initiation sites for plus strands (2, 18, 21) (see Fig. 4). Most plus-strong-stop DNA appears to be paired with 5′ ends of minus strands (Fig. 7A) or with the growing chains at the 3′ ends of the minus strands (Fig. 7B), since it can be digested by *Eco*RI, which requires double-stranded DNA.

Intramolecular DNA transfer of plus-strong-stop DNA (25) can create a partially double-stranded circle (Fig. 7C), which might also serve as a possible intermediate for linear DNA synthesis. However, a side reaction, in which plus-strong-stop DNA is not displaced, may result in single-LTR circular forms (Fig. 7D). Accumulation of plus-strong-stop DNA (Fig. 4) in the infected cells implies that the transfer of plus-strong-stop DNA, which served as the primer for continued plus-strand synthesis and as the template for completion of minus-strand synthesis, may be inefficient. The inhibition of one-LTR circle formation further supports the previous suggestion that one-LTR circles are products of aberrant reverse transcription (18).

Since minus-strand DNA synthesis cannot be completed without the transfer of plus-strong-stop DNA to the 5′ end of the nascent minus strand, the deficit in the amount of 3′ ends of the minus strands may be due to inefficient plus-strong-stop DNA transfer. An alternative explanation for the lack of 3′ ends of the minus strands is slow strand displacement synthesis. Since most plus-strong-stop DNA is paired with the minus-strand DNA template, extension of the 3′ ends of the minus strands would require displacement of this DNA duplex and would occur as slowly and as inefficiently as that of plus strands.

As DNA synthesis proceeds, the full-length plus strands are synthesized, probably by elongation of plus-strong-stop DNA, displacing the internally initiated plus-strand fragments (2, 18) (Fig. 7E). It is also possible that the full-length strands are made by ligation of the short, internally initiated plus-strand fragments.

It has been proposed previously that strand displacement synthesis may require high activation energy (18). Plus-strand DNA synthesis in vitro with detergent-disrupted virions was shown to be slow, and no full-length DNA was found even after minus-strand DNA synthesis was completed (2, 18). In our in vitro integration reaction, however, full-length plus strands were synthesized relatively rapidly, within 1 h. An alternative explanation is that full-length plus-strand synthesis requires a host factor. The lack of

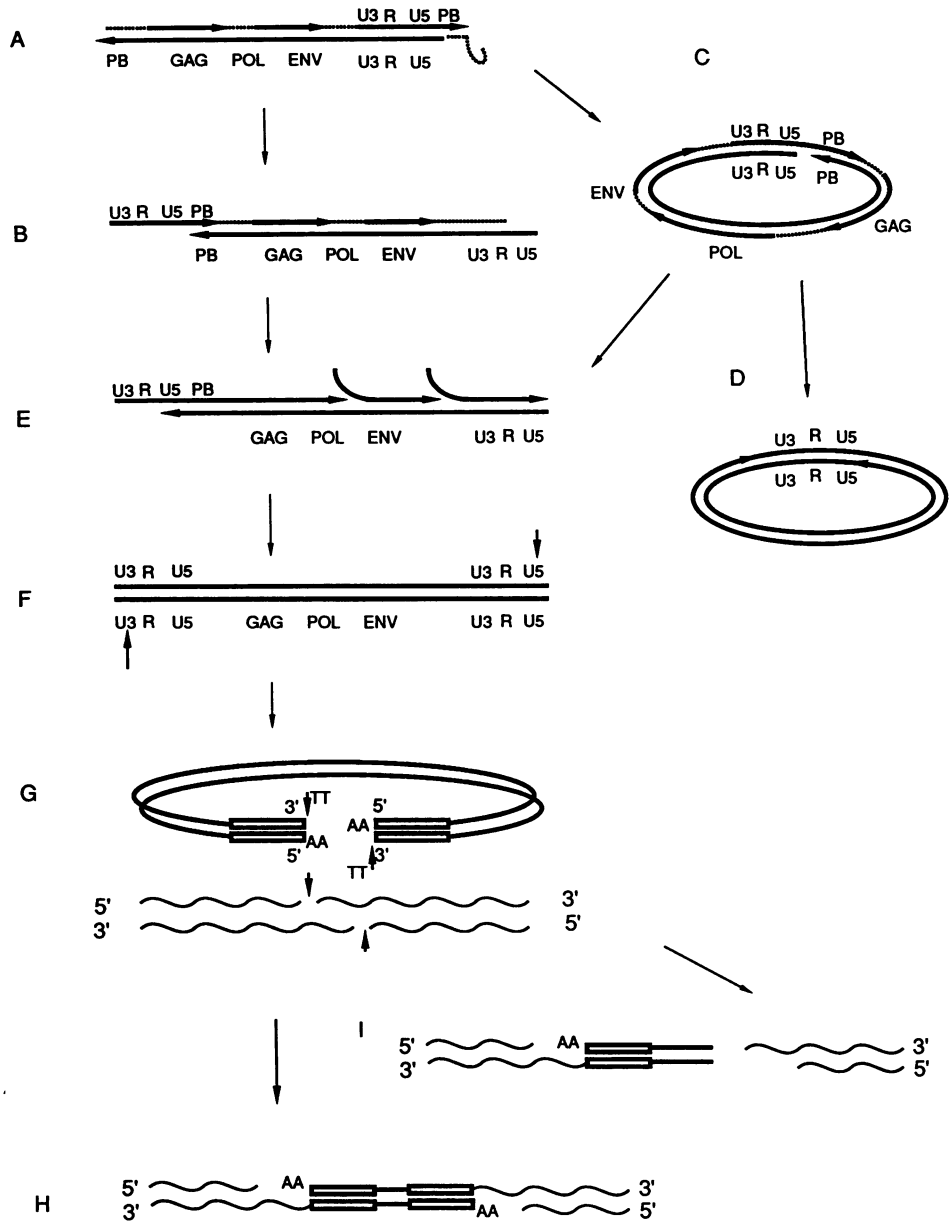

FIG. 7. Overall regulation of avian retrovirus replication in vitro. Details are described in the text under Discussion. The relative sizes of the various regions of the viral genomes are not shown to scale. PB, Primer-binding site.

full-length plus-strand DNA in the infected-cell cytoplasm suggests that a host factor, if there is one, may be of nuclear origin. Although the extract used for our experiments was mainly cytoplasmic, some preexisting supercoiled viral DNA (Fig. 1) and topoisomerase activity (data not shown) in the extract indicate the presence of contaminating nuclear factors.

Following synthesis of the full-length flush-ended linear DNA, 2 nucleotides are cleaved off each 3′ end (Fig. 7F, arrows). Cleavage is probably carried out by the virus-encoded IN protein. The IN protein of avian retroviruses has a specific endonuclease activity and has been shown to remove 2 nucleotides from the 3′ ends of double-stranded linear oligonucleotide substrates which mimic the linear viral termini (20). In MLV, the formation of the recessed ends in vivo requires the presence of IN, and integration is invariably related to generation of recessed ends of the linear DNA (26). The accumulation of cleaved products of viral DNA implies that cleavage of the donor DNA may not be coupled to cleavage and joining of the target DNA. In MLV, it has been clearly shown that cleavage of the donor DNA can be uncoupled from the rest of the integration reaction (13).

Integration of viral DNA into the target occurs by joining of the cleaved 3′ ends to the target DNA (Fig. 7G and H). To generate the target site duplication, LTR ends are presumed to be joined to the 5′ ends of the overhanging strand of staggered-cut target DNA. It has been shown that IN protein can catalyze both cleavage of the target and its joining to viral DNA, at least in vitro (6, 8, 19). A cellular repair system may then complete integration by filling in the gaps, displac-

ing the two mismatched 5′ nucleotides of the LTR, and subsequent ligation (Fig. 7H).

In addition to the complete integration products, some integration products were aberrant structures, with only one LTR joined to the full-length linear φX174 DNA target (Fig. 7I). These molecules could have been generated either by nucleases, which may have cleaved a single-strand integration junction of complete integration products, or, less likely, by preferred integration of viral DNA near the nicks present in the target DNA. It is also possible that these partial integration products were produced by an aberrant integration reaction, in which the joining of one viral DNA end to the target DNA was aborted (perhaps as a result of its incomplete synthesis). The latter possibility would imply that both strands of target DNA were cleaved simultaneously, even when only one strand was joined to the donor viral DNA. We did not observe any structures consisting of an open circle with a linear "tail," resembling those expected from cleavage of one target strand and its joining to an LTR. We are currently analyzing these partial integration products in more detail to determine how they were generated.

Our observations raise a number of interesting questions regarding the synthesis and integration of avian retrovirus DNA. Is viral DNA synthesis a regulatory mechanism for integration? If it is, how is coordination of viral DNA synthesis with integration achieved? If not, why is viral DNA synthesis slow in vivo, and what accelerates it in vitro? Few full-length plus strands were found to accumulate in the avian retrovirus-infected cell cytoplasm (21) or during the in vitro integration reaction. This indicates either that viral DNA synthesis may be a limiting factor for integration or that DNA synthesis may be delayed until appropriate target DNA is present. Integration may occur as soon as viral DNA synthesis is completed in the nucleus. It is also possible that the lack of full-length DNA in the cytoplasm is due to rapid nuclear transport of viral DNA before complete synthesis. If nuclear transport of viral DNA is inhibited, will viral DNA synthesis be completed in the cytoplasm? Further studies are necessary to answer these questions.

ACKNOWLEDGMENTS

We thank Mary Bostic-Fitzgerald for editorial assistance and Wayne Frankel and Terryl Stacy for critical comments on the manuscript.

This work was supported by grants from the National Cancer Institute (CA17659 and CA44385) to J. M. Coffin.

REFERENCES

1. **Benjamin, H., and N. Kleckner.** 1989. Intramolecular transposition by Tn*10*. Cell **59**:373–383.
2. **Boone, L. R., and A. M. Skalka.** 1981. Viral DNA synthesized in vitro by avian retrovirus particles permeabilized with melittin. J. Virol. **37**:109–116.
3. **Bowerman, B., P. O. Brown, J. M. Bishop, and H. E. Varmus.** 1989. A nucleoprotein complex mediates the integration of retroviral DNA. Genes Dev. **3**:469–478.
4. **Brown, P. O., B. Bowerman, H. E. Varmus, and J. M. Bishop.** 1987. Correct integration of retroviral DNA in vitro. Cell **49**:347–356.
5. **Brown, P. O., B. Bowerman, H. E. Varmus, and J. M. Bishop.** 1989. Retroviral integration: structure of the initial covalent product and its precursor, and a role for the IN protein. Proc. Natl. Acad. Sci. USA **86**:2525–2529.
6. **Bushman, F. D., T. Fujiwara, and R. Craigie.** 1990. Retroviral DNA integration directed by HIV integration protein in vitro. Science **249**:1555–1558.
7. **Church, G. M., and W. Gilbert.** 1984. Genomic sequencing. Proc. Natl. Acad. Sci. USA **81**:1991–2008.
8. **Craigie, R., T. Fujiwara, and F. D. Bushman.** 1990. The IN protein of Moloney murine leukemia virus processes the viral DNA ends and accomplishes their integration in vitro. Cell **62**:829–837.
9. **Craigie, R., and K. Mizuuchi.** 1985. Mechanism of transposition of bacteriophage Mu: structure of a transposition intermediate. Cell **41**:867–876.
10. **Eichinger, D. J., and J. D. Boeke.** 1990. A specific terminal structure is required for Ty1 transposition. Genes Dev. **4**:324–330.
11. **Ellison, V., H. Abrams, T. Y. Rose, J. Lifson, and P. Brown.** 1990. Human immunodeficiency virus integration in a cell-free system. J. Virol. **64**:2711–2715.
12. **Finston, W. I., and J. J. Champoux.** 1984. RNA-primed initiation of Moloney murine leukemia virus plus strands by reverse transcriptase in vitro. J. Virol. **51**:26–33.
13. **Fujiwara, T., and R. Craigie.** 1989. Integration of mini-retroviral DNA: a cell-free reaction for biochemical analysis of retroviral integration. Proc. Natl. Acad. Sci. USA **86**:3065–3069.
14. **Fujiwara, T., and K. Mizuuchi.** 1988. Retroviral DNA integration: structure of an integration intermediate. Cell **54**:497–504.
15. **Gilboa, E., S. Mitra, S. Goff, and D. Baltimore.** 1979. A detailed model of reverse transcription and tests of crucial aspects. Cell **18**:93–100.
16. **Grandgenett, D. P., and S. R. Mumm.** 1990. Unraveling retrovirus integration. Cell **60**:3–4.
17. **Hsu, T. W., and J. M. Taylor.** 1982. Single-stranded regions on unintegrated avian retrovirus DNA. J. Virol. **44**:47–53.
18. **Junghans, R. P., L. R. Boone, and A. M. Skalka.** 1982. Products of reverse transcription in avian retrovirus analyzed by electron microscopy. J. Virol. **43**:544–554.
19. **Katz, R. A., G. Merkel, J. Kulkosky, J. Leis, and A. M. Skalka.** 1990. The avian retroviral IN protein is both necessary and sufficient for integrative recombination in vitro. Cell **63**:87–95.
20. **Katzman, M., R. A. Katz, A. M. Skalka, and J. Leis.** 1989. The avian retroviral integration protein cleaves the terminal sequences of linear viral DNA at the in vivo sites of integration. J. Virol. **63**:5319–5327.
21. **Kung, H. J., Y. K. Fung, J. E. Majors, J. M. Bishop, and H. E. Varmus.** 1981. Synthesis of plus strands of retroviral DNA in cells infected with avian sarcoma virus and mouse mammary tumor virus. J. Virol. **37**:127–138.

21a. **Lee, Y. M., and J. M. Coffin.** 1990. Efficient autointegration of avian retrovirus DNA in vitro. J. Virol. **64**:5958–5965.

22. **Maniatis, T., E. F. Fritsch, and J. Sambrook.** 1982. Molecular cloning: a laboratory manual. Cold Spring Harbor Laboratory, Cold Spring Harbor, N.Y.
23. **Moscovici, C., M. G. Moscovici, H. Jimenez, M. M. C. Lai, M. J. Hayman, and P. K. Vogt.** 1977. Continuous tissue culture cell lines derived from chemically induced tumors of Japanese quail. Cell **11**:95–103.
24. **Omer, C., R. Resnick, and A. J. Faras.** 1984. Evidence for involvement of an RNA primer in initiation of strong-stop plus DNA synthesis during reverse transcription in vitro. J. Virol. **50**:465–470.
25. **Panganiban, A. T., and D. Fiore.** 1988. Ordered interstrand and intrastrand DNA transfer during reverse transcription. Science **241**:1064–1069.
26. **Roth, M. J., P. L. Schwartzberg, and S. P. Goff.** 1989. Structure of the termini of DNA intermediates in the integration of retroviral DNA: dependence on IN function and terminal DNA sequence. Cell **58**:47–54.
27. **Schwartz, D. E., R. Tizard, and W. Gilbert.** 1983. Nucleotide sequence of Rous sarcoma virus. Cell **32**:853–869.
28. **Shank, P. R., P. J. Schatz, L. M. Jensen, P. N. Tsichlis, J. M. Coffin, and H. L. Robinson.** 1985. Sequences in the gag-pol-5′env region of avian leukosis viruses confer the ability to induce osteopetrosis. Virology **145**:94–104.
29. **Shih, C.-C., J. P. Stoye, and J. M. Coffin.** 1988. Highly preferred targets for retrovirus integration. Cell **53**:531–537.

30. **Smith, J., A. Cywinski, and J. Taylor.** 1984. Initiation of plus-strand DNA synthesis during reverse transcription of an avian retrovirus genome. J. Virol. **49**:200–204.
31. **Sutcliffe, J. G.** 1978. Complete nucleotide sequence of the *Escherichia coli* plasmid pBR322. Cold Spring Harbor Symp. Quant. Biol. **43**:77–90.
32. **Swanstrom, R., J. M. Bishop, and H. E. Varmus.** 1982. Structure of a replication intermediate in the synthesis of Rous sarcoma virus DNA in vivo. J. Virol. **42**:337–341.
33. **Varmus, H., and P. Brown.** 1989. Retroviruses, p. 53–108. *In* M. Howe and D. Berg (ed.), Mobile DNA. American Society for Microbiology, Washington, D.C.